Journal of Organometallic Chemistry 1021 (2024) 123356

Contents lists available at ScienceDirect

Journal of Organometallic Chemistry

journal homepage: www.elsevier.com/locate/jorganchem

Selectivity control in the reactivity of dipyrromethene gallium(I) complexes

Tim Richter, Stefan Thum, Oliver P.E. Townrow, Jens Langer, Michael Wiesinger, Sjoerd Harder *

Inorganic and Organometallic Chemistry, Friedrich-Alexander Universität Erlangen-Nürnberg, Egerlandstraße 1, 91058, Erlangen, Germany

ARTICLE INFO

Keywords:
Gallium
Low-valent
Dipyrromethene ligand
Imido
Azide

ABSTRACT

Following the recent isolation and structural characterization of the first low-valent Ga^I complex with a monoanionic dipyrromethenide ligand (DPM), herein (DPM)Ga^I complexes with bulky aryl-substituents in the 1- and 9-positions are described. This study focusses on three DPM ligands with mesityl substituents (^{Mes}DPM), 2,6-diisopropylphenyl substituents (^{DIPP}DPM), or 10-isopropyl-9-anthracenyl substituents ($^{i\text{Pr-Anth}}$DPM); the synthesis to the latter unknown ligand is described. The precursors (^{R}DPM)GaI_2 were obtained by reaction of the corresponding alkali metal complexes (^{R}DPM)M (*M* = Na or K) with GaI_3 and characterized by X-ray diffraction. Crystal structures show the efficient shielding of the GaI_2 unit by two flanking aryl groups. In a subsequent reduction step, (^{DIPP}DPM)Ga^I and ($^{i\text{Pr-Anth}}$DPM)Ga^I have been isolated. Comparison of the crystal structure of (^{DIPP}DPM)Ga^I with that of a similar β-diketiminate Ga^I complex shows that the Ga center in the DPM complex is well shielded by flanking DIPP substituents. Despite this favorable ligand geometry, isolation of the corresponding (DPM)Ga=*N*($SiMe_3$) complexes failed due to further reaction with a second equivalent of Me_3SiN_3. This resulted in clean formation of the tetrazagallole complex ($^{t\text{Bu}}$DPM)Ga[$N_4(SiMe_3)_2$] and the amide/azide combination ($^{i\text{Pr-Anth}}$DPM)Ga(N_3)N($SiMe_3$)$_2$, both structurally characterized by X-ray diffraction. Selective formation of both complexes shows that the substituents in the DPM ligand effectively control the course of the reaction. DFT calculations show that independent of the substituent (*t*Bu, DIPP, or *i*Pr-Anth) the amide/azide combination is always *circa* 20 kcal/mol more stable than the tetrazagallole product. The latter must therefore be formed by kinetic control.

1. Introduction

The carbene-like reactivity of Al^I and related Ga^I complexes has been extensively documented [1,2,3]. High-lying filled HOMO and low-lying vacant LUMO orbitals at a single metal center define the versatile transition metal-like reactivity of these reagents [4,5]. Most reactivity studies on such low-valent complexes are centered around their β-diketiminate complexes with the ubiquitously used ^{DIPP}BDI ligand (**I**, Scheme 1) [2]. Synthetic routes to such BDI complexes generally give very poor yields due to decomposition [6,7,8,9]. We recently showed that using the considerably larger ^{DIPeP}BDI ligand (**II**) contributes significantly to their stabilities and, as a result, the Al^I and Ga^I complexes could be obtained essentially in quantitative yield [10,11].

In our most recent contribution, we considered the dipyrromethene ligand (DPM) for stabilization of group 13 metal centers [12]. Although this ligand is very popular for application in highly fluorescent boron complexes (BODIPYs) [13], remarkably no heavier group 13 metal complexes were known. In comparison to BDI ligands, the DPM ligands encapsulate the metal considerably more efficiently. Attempts to isolate a (DPM)Al^I complex failed, most likely because the extensively conjugated π-system in such ligands can be easily reduced by the Al^I center. However, the significantly larger HOMO-LUMO gap in Ga^I complexes enabled the isolation of the slightly less reactive (DPM)Ga^I which crystallized as a dinuclear complex (**III**) [12]. As **III** is monomeric in benzene solution, the Ga-Ga bond is weak. In fact, **III** is mainly kept together by dispersive interactions [12].

We now extend our previous research on (DPM)Ga^I complexes by increasing the bulk of the flanking substituents in the 1- and 9-positions of the DPM ligand. We aimed to isolate (DPM)Ga^I reagents that potentially could be converted to monomeric Ga imido complexes of type (DPM)Ga=NR in which the Ga=NR bond is well shielded, avoiding further aggregation. Such monomeric Ga-imido complexes are expected

* Corresponding author.
E-mail address: sjoerd.harder@fau.de (S. Harder).
@harder_research (S. Harder)

https://doi.org/10.1016/j.jorganchem.2024.123356
Received 5 June 2024; Received in revised form 2 September 2024; Accepted 4 September 2024
Available online 4 September 2024

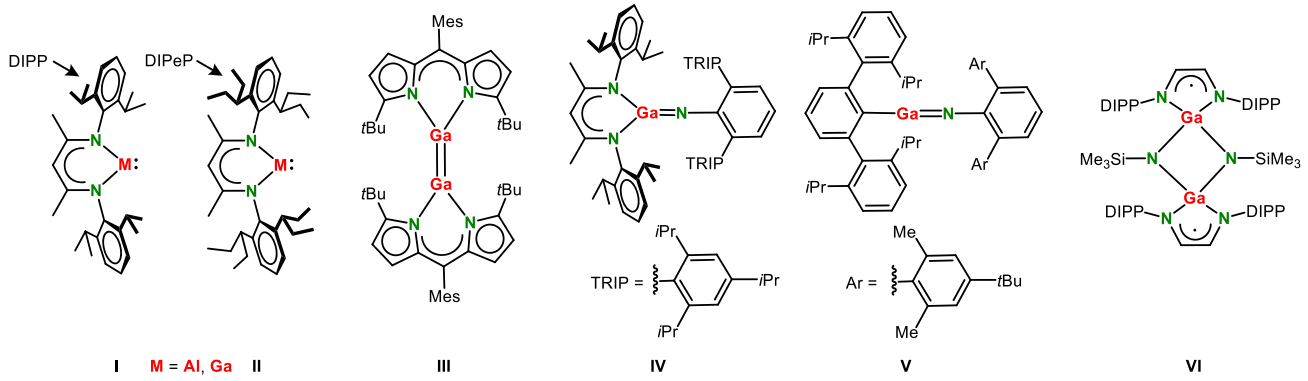

Scheme 1. Selected Ga^{I} and Ga-imido complexes.

to show very high reactivities. Earlier reports by Power and coworkers describe the successful isolation of Ga imido complexes with extremely bulky R-substituents at N (**IV-V**) [14,15], resulting in near linear Ga=*N*-R geometries. Jones and coworkers showed that smaller substituents, like the Me_3Si-group, resulted in stabilization by dimerization (**VI**), compromising its reactivity [16]. In this work we describe the synthesis of a hitherto unknown DPM-ligand and new (DPM)Ga^{I} reagents and discuss our attempts to stabilize (DPM)Ga=*N*($SiMe_3$) complexes with bulky DPM ligands.

2. Results and discussion

We consider three different DPM ligands featuring substituents of increasing steric bulk in the 1- and 9-positions. ^{Mes}DPM and ^{DIPP}DPM could be obtained according to reported routes [17,18]. The largest, hitherto unreported ligand $^{iPr\text{-}Anth}$DPM was prepared using a similar route (Scheme 2a) and is a variation on the previously reported ^{Anth}DPM ligand [19]. As complexes of the latter ligand with anthracenyl substituents are generally quite insoluble, the *i*Pr group was introduced to improve solubility.

The syntheses of the low-valent Ga^{I} complexes followed the same pathway as previously reported for (^{tBu}DPM)Ga (Scheme 2b) [12]. The ligands were first deprotonated with commercially available MN($SiMe_3$)$_2$ (*M* = Na or K) in benzene to give the corresponding (^{R}DPM)M complexes in essentially quantitative yield, either as orange-red powders (*R* = Mes, DIPP) or as a deep purple powder (*R* = *i*Pr-Anth). Crystal structures and selected bond distances for the monomeric complexes (^{DIPP}DPM)K·(η^6-toluene) and ($^{iPr\text{-}Anth}$DPM)Na·(THF)$_2$ and are shown in Fig. 1.

In a subsequent salt-metathesis step, these metal salts were reacted with GaI_3 in benzene to give the corresponding (^{R}DPM)GaI_2 complexes as red (*R* = Mes, DIPP) or purple (*R* = *i*Pr-Anth) powders in yields varying from 65 to 88 %. The crystal structures of all three complexes were determined by X-ray diffraction (Fig. 2) and their geometries compared to that of previously reported (^{tBu}DPM)GaI_2 (Table 1). All complexes have several characteristic features in common. The DPM ligand is not fully planar but slightly distorted in a butterfly geometry (the two C_4N rings are not coplanar). The Ga atom is located slightly outside the NCCCN least-squares plane. One of the iodide ligands is close to the NCCCN plane whereas the other lies well outside this plane. The Ga-N and Ga-I distances are essentially very similar and not sensitive to the bulk or nature of the R-substituent. However, there are differences in the N-Ga-N bite angles which are considerably smaller for (^{Ar}DPM)GaI_2 complexes (94.7(1)−96.4(2)°) when compared to that in (^{tBu}DPM)GaI_2 (101.8(1)°).

In a third step, the Ga iodide precursors were reduced with KC_8 in an aromatic solvent to give the corresponding low-valent Ga^{I} complexes. Using various solvents and methods (solution or mechanochemical), we have not been able to isolate any product in the case of *R* = Mes. However, (^{DIPP}DPM)Ga^{I} and ($^{iPr\text{-}Anth}$DPM)Ga^{I} could be obtained as dark-red and purple powders in quantitative yields. Although the reduction process was carried out at 50 °C and needed prolonged reaction times (1–3 days), the isolated pure complex (^{DIPP}DPM)Ga^{I} decomposes slowly at room temperature, either in solution or as a solid, and therefore needs to be stored at −20 °C. In contrast, a solution of ($^{iPr\text{-}Anth}$DPM)Ga^{I} in benzene did not show any signs of decomposition, even when heated for 24 h at 70 °C. Therefore, the bulk of the substituents at the pyrrole rings seems to have a large effect on complex stability.

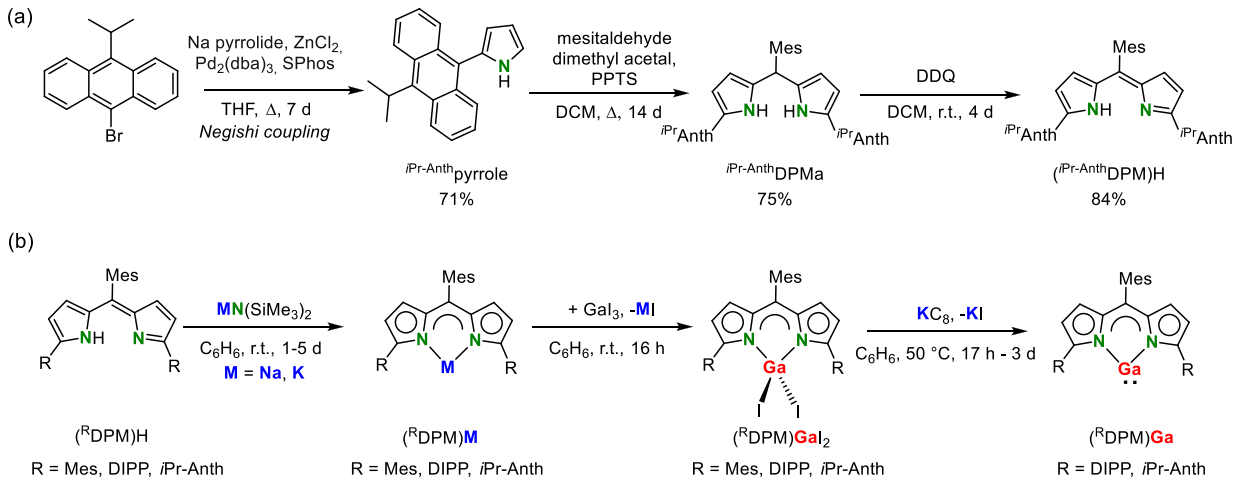

Scheme 2. Synthesis of the ($^{iPr\text{-}Anth}$DPM)H ligand (a) and the (^{R}DPM)GaI_2 and (^{R}DPM)Ga^{I} complexes (b).

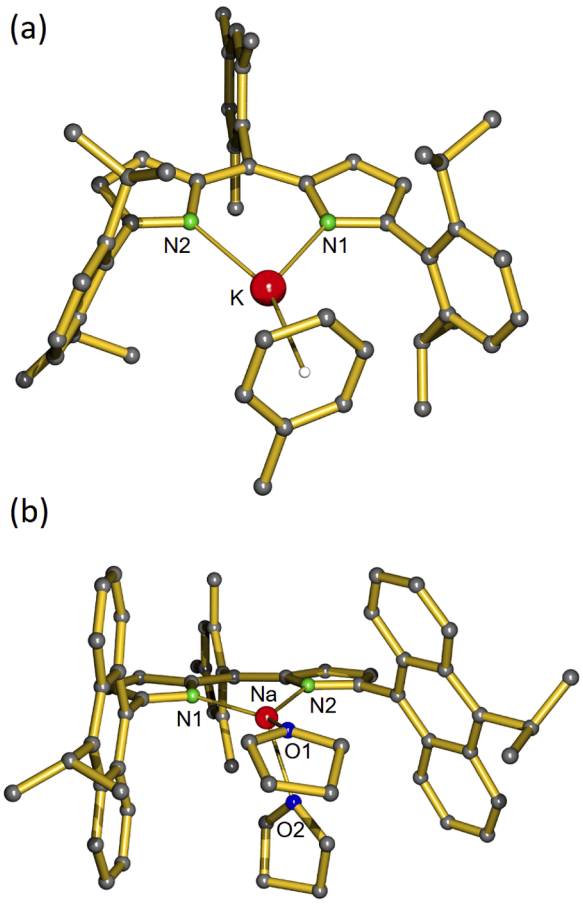

Fig. 1. Crystal structures of DPM alkali metal complexes; selected bond distances in Å and H atoms omitted for clarity. (a) (^{DIPP}DPM)K·(toluene): K-N1 2.683(5), K-N2 2.640(5), K-C(toluene) 3.171(6)–3.419(5) (average 3.280), K-ring(centroid) 2.975(3). (b) ($^{iPr\text{-}Anth}$DPM)Na·(THF)$_2$: Na-N1 2.336(1), Na-N2 2.320(1), Na-O1 2.248(1), Na-O2 2.320(1).

Complex (^{DIPP}DPM)Ga^{I} is highly soluble in non-polar solvents and was crystallized from hexane at −35 °C in the form of dark-red cubes suitable for X-ray diffraction. Complex ($^{iPr\text{-}Anth}$DPM)Ga^{I} does not dissolve in alkanes and is only sparingly soluble in aromatic solvents. However, it dissolves well in THF in which it is stable. Using different solvents and methods, we have not been able to recrystallize ($^{iPr\text{-}Anth}$DPM)Ga^{I}.

In contrast to the dimeric structure of (^{tBu}DPM)Ga^{I} [12], which is weakly bound by a Ga-Ga interaction and additional dispersive forces between the DPM ligands, the crystal structure of (^{DIPP}DPM)Ga^{I} (Fig. 3) is mononuclear. These different aggregation states influence the geometries of the (DPM)Ga framework (see Table 1 for comparison). Compared to (^{tBu}DPM)Ga^{I}, the DPM ligand in (^{DIPP}DPM)Ga^{I} is much flatter and the Ga atom resides closer to the NCCCN least-squares plane.

Direct comparison of (^{DIPP}DPM)Ga^{I} with the corresponding β-diketiminate complex (^{DIPP}BDI)Ga^{I} [8] (Fig. 3), shows that the Ga^{I} center in the DPM complex is sandwiched between the DIPP-substituents. Although the shortest distances to the Ga center are relatively long (Ga-C$_{ipso}$ 3.289(3)/3.235(3) Å), the Ga atom is highly shielded in a cleft formed by the DIPP-rings which make an angle of 37.5(1)° with each other. For comparison, the rings in (^{DIPP}BDI)Ga^{I} make an angle of 125.4 (1)°. Differences in shielding of the Ga center is especially noticeable in a comparison of space-filling models for both structures (Fig. 3b). Interestingly, calculating the buried volume with default parameters (3.5 Å sphere, no H atoms) gives exactly the same numbers for (^{DIPP}DPM)Ga^{I} and (^{DIPP}BDI)Ga^{I} (V$_{bur}$ = 58.8 %) [20] (Fig. 3c). However, choosing the larger radius around the metal of 4.5 Å shows a significantly larger buried volume for (^{DIPP}DPM)Ga^{I} (62.2 %) than for (^{DIPP}BDI)Ga^{I} (59.5 %). This is a clear demonstration for the remote shielding capabilities of the DPM ligand. Similar remote shielding of Ga^{I} centers has been found in complexes with a 1,8-substituted carbazole ligand [21] or a *bis* (4-benzhydryl-benzoxazol-2-yl)methanide ligand [22]. Although we have not been able to structurally characterize ($^{iPr\text{-}Anth}$DPM)Ga^{I}, it can be anticipated that the coordination sphere around the Ga metal is confined between two larger anthracenyl-substituents. Such systems are attractive candidates for isolation of complexes with isolated Ga=NR bonds.

The reaction of the two new low-valent complexes (^{DIPP}DPM)Ga^{I} and ($^{iPr\text{-}Anth}$DPM)Ga^{I} with Me_3SiN_3 in benzene at room temperature is instantaneous. Using a 1:1 stoichiometric ratio, half of the Ga^{I} complex remains unreacted. This suggests that two equivalents of Me_3SiN_3 are needed for full conversion. Indeed, similar to the reaction of (^{DIPP}BDI)Ga^{I} with Me_3SiN_3 [23] the highly reactive imido intermediate reacts further with a second equivalent of Me_3SiN_3 (Scheme 3). Interestingly, (^{DIPP}BDI)Ga^{I} reacted with Me_3SiN_3 to give two different products which are structural isomers: the amide/azide combination (^{DIPP}BDI)Ga(N$_3$)N(SiMe$_3$)$_2$ and the tetrazagallole (^{DIPP}BDI)Ga[N$_4$(SiMe$_3$)$_2$] in 3:1 ratio. With the DPM ligands ^{tBu}DPM and ^{DIPP}DPM, only tetrazagallole products are formed (the raw products are essentially clean and do not show ^{1}H NMR signals for the amide/azide combination). However, in case of ($^{iPr\text{-}Anth}$DPM)Ga^{I} only the amide/azide combination was observed. This not only shows that reactions with (DPM)Ga^{I} reagents are much more selective than those with (BDI)Ga^{I} but also demonstrates that changing the substituents in the DPM ligand can have a tremendous effect on product selectivity.

The products (^{DIPP}DPM)Ga[N$_4$(SiMe$_3$)$_2$] and ($^{iPr\text{-}Anth}$DPM)Ga(N$_3$)N(SiMe$_3$)$_2$ were structurally characterized (Fig. 4). The structure of the tetrazagallole complex (^{DIPP}DPM)Ga[N$_4$(SiMe$_3$)$_2$] resembles that of previously reported (^{tBu}DPM)Ga[N$_4$(SiMe$_3$)$_2$] showing similar Ga-N distances and a N—*N* = *N*—N backbone in the N$_4$-unit [12]. The structure of the amide/azide combination ($^{iPr\text{-}Anth}$DPM)Ga(N$_3$)N(SiMe$_3$)$_2$ resembles that of previously reported β-diketiminate or DPM complexes with this anion combination [23,11,12] showing a similar Ga coordination geometry. The significantly unequal N—N bond lengths in the azide anion indicate that the Ga-N-N≡N resonance structure dominates the structure.

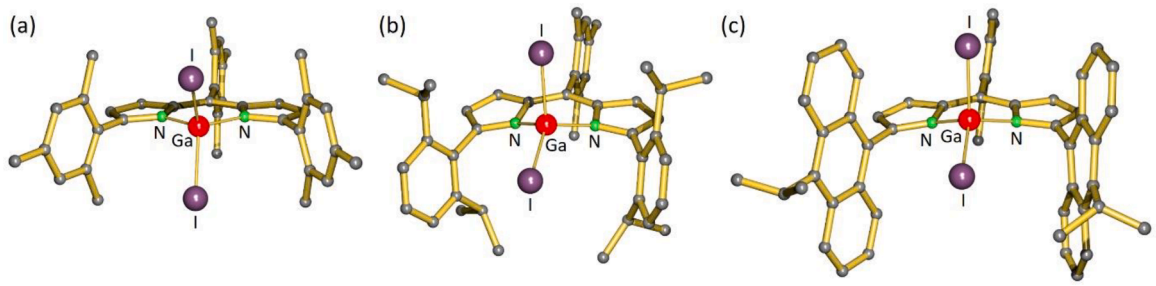

Fig. 2. Crystal structures of (a) (^{Mes}DPM)GaI$_2$, (b) (^{DIPP}DPM)GaI$_2$ and (c) ($^{iPr\text{-}Anth}$DPM)GaI$_2$; H atoms omitted for clarity.

Table 1
Selected geometric parameters for (^{R}DPM)GaI$_2$ and (^{R}DPM)Ga complexes (distances in Å and angles in degrees). Values for complexes with the ^{tBu}DPM ligand are taken from ref. [12].

Complex	(^{R}DPM)GaI$_2$				(^{R}DPM)Ga	
	R = *t*Bu	R = Mes	R = DIPP	R = *i*Pr-Anth	R = *t*Bu[c]	R = DIPP
Ga-N	1.951(2)–1.958(2)	1.945(6)	1.928(2)–1.934(2)	1.934(2)–1.937(2)	2.053(1)-2.056(1)	2.095(2)–2.105(2)
Ga-I	2.5270(5)–2.5467(6)	2.514(2)–2.519(1)	2.478(8)–2.537(4)	2.4828(5)–2.5232(5)	–	–
N-Ga-N	101.8(1)	96.4(2)	94.66(8)	95.33(7)–95.72(7)	87.89(5)	83.76(9)
I-Ga-I	114.76(2)	109.23(5)	115.11(2)	115.30(2)–115.97(2)	–	–
C_4N/C_4N[a]	9.4(2)		11.9(2)	8.89(12)–11.63(13)	16.9(1)°	7.30(17)
Ga/NCCCN [b]	0.439(1)	0.015(1)	0.678(1)	0.5956(3)–0.6131(4)	0.909(1)	0.1732(4)

[a] Dihedral angle between the least-squares planes of the five-membered C_4N rings.
[b] Distance of the Ga metal from the NCCCN least-squares plane.
[c] Dinuclear structure.

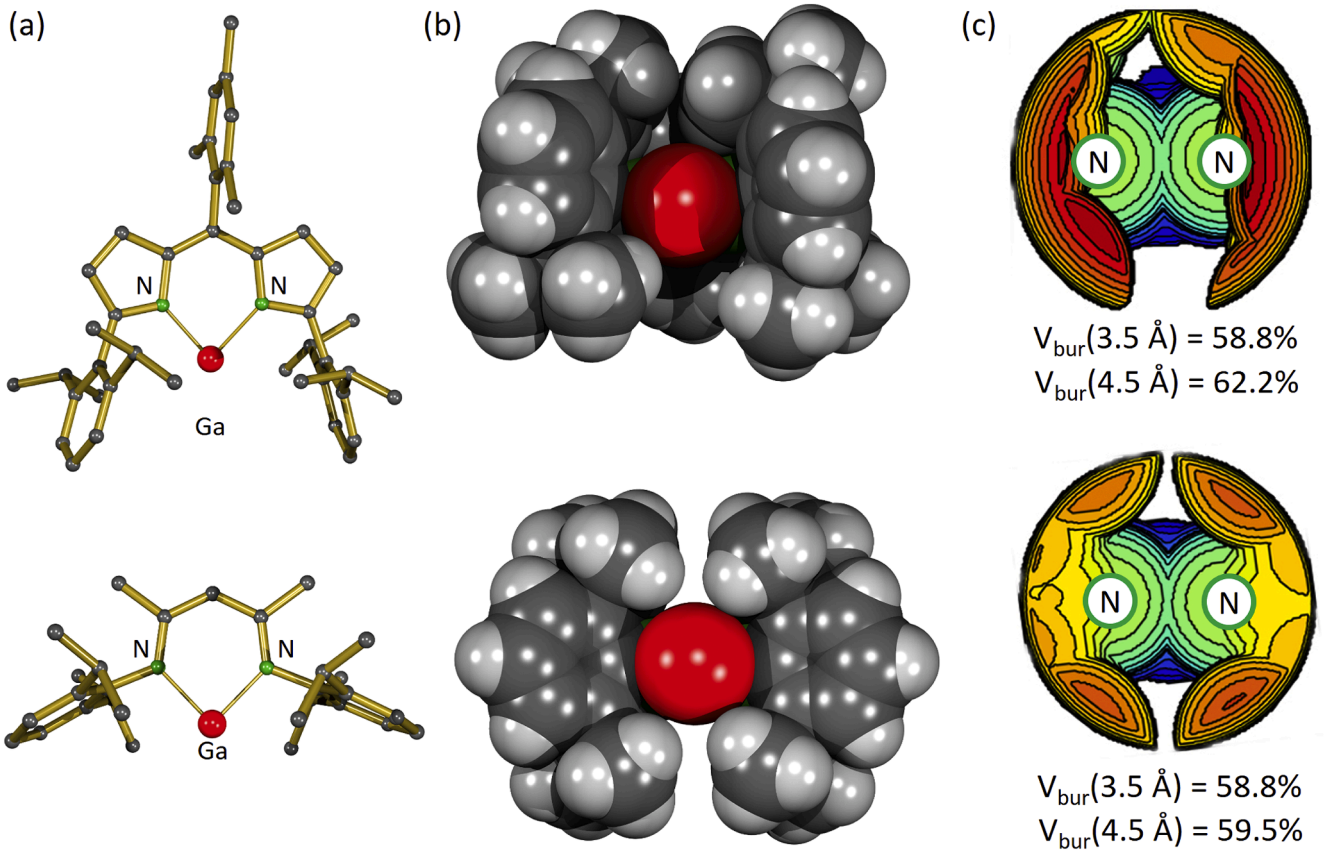

Fig. 3. Comparison of the crystal structure of (^{DIPP}DPM)Ga^{I} (top) with that of (^{DIPP}BDI)Ga^{I} (bottom). (a) Ball and stick models (H atoms omitted for clarity). (b) Space-filling models (frontal view). (c) Buried volume (3.5 and 4.5 Å radius, atomic radii scaled by 1.17, no H atoms).

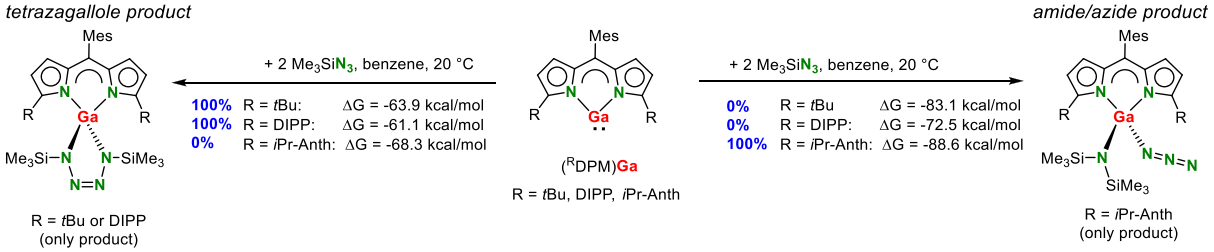

Scheme 3. Reaction of (^{R}DPM)Ga^{I} complexes with Me_3SiN_3 to give two different products. Shown are the selectivities (blue) and the calculated Gibbs free energies (298 K) for the different substituents R.

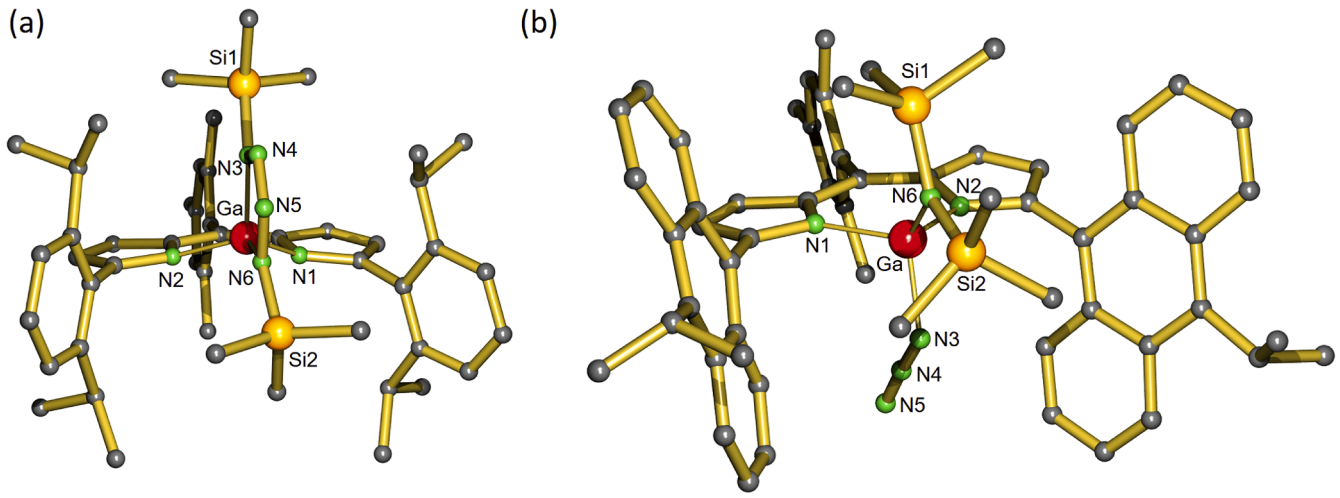

Fig. 4. Crystal structures of tetrazagallole and gallium amide/azide complexes; selected bond distances in Å and H atoms omitted for clarity. (a) (^{DIPP}DPM)Ga[$N_4(SiMe_3)_2$]: Ga-N1 1.961(1), Ga-N2 1.960(1), Ga-N3 1.891(1), Ga-N6 1.855(1), N3-N4 1.396(2), N4-N5 1.263(2), N5-N6 1.401(2). (b) Ga-N1 1.973(2), Ga-N2 1.968(2), Ga-N3 1.909(2), Ga-N6 1.852(2), N3-N4 1.221(2), N4-N5 1.143(2).

DFT calculations (PBE0-D3BJ/Def2-TZVP; PCM = Benzene) show the Gibbs free energy changes for reaction of (^{R}DPM)Ga^{I} complexes with two equivalents of Me_3SiN_3 (Scheme 3). For all substituents (R = *t*Bu, DIPP, and *i*Pr-Anth) the formation of the amide/azide combination (^{R}DPM)Ga(N_3)N($SiMe_3$)$_2$ is clearly favored. Since we found that the tetrazagallole and amide/azide products do not interconvert into each other, also not after heating to 100 °C in toluene, the formation of the less stable tetrazagallole products (for R = *t*Bu and DIPP) must be kinetically favored instead of thermodynamically controlled.

3. Conclusion

Two new low-valent Ga^{I} complexes, (^{DIPP}DPM)Ga^{I} and ($^{i\text{Pr-Anth}}$DPM)Ga^{I}, could be obtained in near quantitative yields by reduction of the corresponding (DPM)GaI_2 precursors. The crystal structure of (^{DIPP}DPM)Ga^{I} shows efficient shielding of the Ga metal center and therefore these represent the first monomeric dipyrromethenide Ga^{I} complexes. The structure of the similar β-diketiminate complex (^{DIPP}DPM)Ga^{I} features a much more open metal coordination. Based on the protection of the metal centers in (DPM)Ga^{I} complexes, it was anticipated that reaction with Me_3SiN_3 could give stable monomeric Ga imido complexes: (DPM)Ga=*N*($SiMe_3$). However, reaction with a second equivalent of Me_3SiN_3 led to clean formation of either the tetrazagallole complex ($^{t\text{Bu}}$DPM)Ga[$N_4(SiMe_3)_2$] or the amide/azide combination ($^{i\text{Pr-Anth}}$DPM)Ga(N_3)N($SiMe_3$)$_2$. Since the reaction of the β-diketiminate complex (^{DIPP}BDI)Ga^{I} with Me_3SiN_3 gave a mixture of products, (^{R}DPM)Ga^{I} complexes react remarkably more selective. The substituents in the DPM ligand effectively control the course of the reaction. DFT calculations show that, independent of the substituent (*t*Bu, DIPP, or *i*Pr-Anth), the amide/azide combination is always *circa* 10–20 kcal/mol more stable than the tetrazagallole product. Since both products do not interconvert into each other (also not after heating), tetrazagallole formation must be kinetically controlled.

4. Experimental

4.1. General procedures

All experiments were conducted under an inert atmosphere by applying standard Schlenk techniques or using nitrogen-filled gloveboxes (MBraun, Labmaster SP). Benzene, hexanes, *n*-pentane, THF, and toluene were degassed with nitrogen and dried over activated aluminum oxide (Innovative Technology, Pure Solv 400–4-MD, Solvent Purification System) and stored under inert atmosphere over molecular sieves (3 Å). Chlorobenzene, dichloromethane, *N,N*-dimethylformamide, and fluorobenzene were dried over calcium hydride, distilled under N_2 atmosphere and stored over 3 Å molecular sieves. $CDCl_3$ (Sigma Aldrich), CD_2Cl_2 (Sigma-Aldrich), C_6D_6 (Sigma Aldrich), THF-d_8 (99.6 % D, Sigma-Aldrich), and toluene-d_8 (Sigma Aldrich) were dried over 3 Å molecular sieves. Anthrone (Alfa Aesar), (2-biphenyl)di-*tert*-butylphosphine (JohnPhos 97 %, Sigma-Aldrich), 2-bromo-mesitylene (TCI Chemicals), 2-bromopropane (Acros Organics), (1*S*)-(+)−10-camphorsulfonic acid (Sigma-Aldrich), 2,3-dichloro-5,6-dicyano-1,4-benzoquinone (DDQ, abcr), 2-dicyclohexylphosphino-2′,6′-dimethoxybiphenyl (SPhos, Sigma-Aldrich), gallium (99.99 %, 2lab Laborfachhandel), graphite (99.9 %, abcr), magnesium (Alfa Aesar), mesitaldehyde (abcr), *N*-bromosuccinimide (NBS, Sigma-Aldrich), potassium (chunks, washed with hexanes, 98 % trace metal basis, Sigma-Aldrich), potassium *bis*(trimethylsilyl)amide (anhydrous 95 %, Sigma-Aldrich), pyridinium *p*-toluenesulfonate (PPTS, TCI Chemicals), sodium *bis*(trimethylsilyl)amide (95 %, Sigma-Aldrich), trimethylsilyl azide (95 %, abcr), trimethyl *ortho*-formate (Alfa Aesar), *tris*(dibenzylideneacetone)dipalladium(0) ($Pd_2(dba)_3$, 97 %, Sigma-Aldrich), trimethylsilyl azide (anhydrous 95 %, abcr), and $ZnCl_2$ (anhydrous 98 %, abcr) were purchased as indicated and used without further purification. 9-Bromo-10-isopropylanthracene [24], 1,9-di-isopropylphenyl-5-mesityldipyrromethene (^{Dipp}DPM)H [18], gallium(III) triiodide [25], mesitaldehyde dimethyl acetal [26], potassium graphite (KC_8) [27], K/KI [28], sodium pyrrol-1-ide [29], and 1,5,9-trimesityldipyrromethene (^{Mes}DPM)H [17] were prepared according to literature procedures. NMR spectra were recorded with a Bruker Avance III HD 600 MHz NMR spectrometer. Chemical shifts (δ) were reported in parts per million (ppm) and the spectra were referenced to solvent residual signal. Coupling constants (J) were given in Hertz (Hz). Elemental analysis was performed with a Hekatech Eurovector EA 3000 analyzer. All crystal structures were measured on a SuperNova diffractometer with dual Cu and Mo microfocus sources and an Atlas S2 detector.

4.2. Preparations

4.2.1. α-(10-isopropylanthracen-9-yl)−1H-pyrrole ($^{i\text{Pr-Anth}}$pyrrole)

To a mixture of sodium pyrrol-1-ide (5.73 g, 64.3 mmol, 3.20 eq.) and $ZnCl_2$ (8.76 g, 64.3 mmol, 3.20 eq.) in THF (250 mL) were added $Pd_2(dba)_3$ (184 mg, 201 μmol, 1 mol %), SPhos ($C_{26}H_{35}O_2P$, 165 mg, 402 μmol, 2 mol %), and 9-bromo-10-isopropylanthracene (6.00 g, 20.1 mmol, 1.00 eq.) in a Schlenk flask. After refluxing the dark suspension

for 7 days, the reaction mixture was allowed to cool to room temperature and was quenched with a mixture of H_2O (200 mL) and Et_2O (200 mL). The phases were separated and the aqueous phase was extracted with Et_2O (3 × 100 mL). The combined organic phases were washed with a saturated $NaHCO_3$ solution (3 × 100 mL). Drying the organic phase over $MgSO_4$ and removing the solvent under reduced pressure afforded a crude black solid, which was washed with n-hexane (100 mL). Eluting the mixture through a plug of silica gel using DCM as eluent yielded an orange-brown solid, which after recrystallization from a saturated EtOH solution at 4 °C and drying *in vacuo* was isolated as a microcrystalline orange solid consisting of $^{i\text{Pr-Anth}}$pyrrole (4.08 g, 14.3 mmol, 71 %). ^{1}H NMR (C_6D_6, 600 MHz, 298 K): δ = 8.39 (br s, 2H, anthracene-aryl-H), 8.02 (d, J = 8.7 Hz, 2H, anthracene-aryl-H), 7.30 – 7.26 (m, 2H, anthracene-aryl-H), 7.20 – 7.17 (m, 2H, anthracene-aryl-H), 6.60 – 6.59 (m, 1H, pyrrole-H), 6.53 – 6.52 (m, 1H, pyrrole-H), 6.50 – 6.49 (m, 1H, pyrrole-H), 4.47 (sept, J = 7.4 Hz, 1H, $CH(CH_3)_2$), 1.68 (d, J = 7.3 Hz, 6H, $CH(CH_3)_2$) ppm. ^{13}C{^{1}H} NMR (C_6D_6, 151 Hz, 298 K): δ = 141.4 (anthracene-aryl-C), 133.1 (anthracene-aryl-C), 129.6 (anthracene-aryl-C), 129.1 (anthracene-aryl-C), 128.8 (anthracene-aryl-CH), 128.4 (anthracene-aryl-CH), 128.0 (pyrrole-C), 125.0 (anthracene-aryl-CH), 118.0 (pyrrole-CH), 111.6 (pyrrole-CH), 109.2 (pyrrole-CH), 28.8 ($CH(CH_3)_2$), 23.0 ($CH(CH_3)_2$) ppm.

4.2.2. $^{iPr\text{-}Anth}$DPMa

To a solution of $^{i\text{Pr-Anth}}$pyrrole (4.08 g, 14.3 mmol, 1.00 eq.) and mesitaldehyde dimethyl acetal (1.39 g, 7.15 mmol, 0.50 eq.) in DCM (100 mL) in a Schlenk flask was added PPTS (359 mg, 1.43 mmol, 0.10 eq.). After refluxing the suspension for 14 days, the resulting brown solution was filtered through a plug of silica gel using DCM/hexanes in a ratio of 3:1 as eluent. All volatiles were removed *in vacuo* and the brownish oil was triturated twice with hexanes (30 mL). The solvent was removed under reduced pressure and the product dried *in vacuo*, giving $^{i\text{Pr-Anth}}$DPMa as a brown powder (3.74 g, 5.34 mmol, 75 %). ^{1}H NMR (C_6D_6, 600 MHz, 298 K): δ = 8.40 (br s, 3H, anthracene-aryl-*H*), 8.22 (d, *J* = 8.7 Hz, 3H, anthracene-aryl-*H*), 7.51 (s, 2H, anthracene-aryl-*H*), 7.30 – 7.25 (m, 4H, anthracene-aryl-*H*), 7.24 – 7.18 (m, 4H, anthracene-aryl-*H*), 6.77 (s, 2H, Mes-aryl-*H*), 6.46 (t, *J* = 2.9 Hz, 2H, pyrrole-*H*), 6.40 (t, *J* = 2.6 Hz, 2H, pyrrole-*H*), 5.83 (s, 1H, Mes*CH*(C_4H_2 $^{i\text{Pr}}$AnthNH)$_2$), 4.48 (sept, *J* = 7.1 Hz, 2H, *CH*(CH_3)$_2$), 2.33 (s, 6H, *para*-C_6H_2(*CH*$_3$)$_3$), 2.11 (s, 3H, *ortho*-C_6H_2(*CH*$_3$)$_3$), 1.70 (d, *J* = 7.3 Hz, 12H, CH(*CH*$_3$)$_2$) ppm (N*H* protons not found). ^{13}C{^{1}H} NMR (C_6D_6, 151 Hz, 298 K): δ = 141.4 (anthracene-aryl-*C*), 137.7 (anthracene-aryl-*C*), 136.4 (Mes-aryl-*C*), 135.5 (Mes-aryl-*C*), 133.2 (anthracene-aryl-*C*), 132.6 (pyrrole-*C*), 130.8 (Mes-aryl-*C*H), 130.7 (anthracene-aryl-*C*), 129.7 (anthracene-aryl-*C*), 129.2 (anthracene-aryl-*C*), 128.6 (anthracene-aryl-*C*H), 127.1 (pyrrole-*C*), 125.1 (anthracene-aryl-*C*H), 125.0 (anthracene-aryl-*C*H), 112.0 (pyrrole-*C*H), 109.6 (Mes-aryl-*C*H), 108.3 (pyrrole-*C*H), 39.6 (Mes*C*H(C_4H_2 $^{i\text{Pr}}$AnthN)$_2$), 28.8 (*C*H(CH_3)$_2$), 23.0 (CH(*C*H$_3$)$_2$), 21.2 (*para*-C_6H_2(*C*H$_3$)$_3$), 20.8 (*ortho*-C_6H_2(*C*H$_3$)$_3$ ppm.

4.2.3. $^{iPr\text{-}Anth}$DPM-H

The oxidant DDQ (1.61 g, 7.11 mmol, 1.10 eq.) was added to a solution of $^{i\text{Pr-Anth}}$DPMa (4.53 g, 6.46 mmol, 1.00 eq.) in DCM (60 mL) in a Schlenk flask and the reaction mixture immediately turned dark purple whereupon it was stirred at room temperature for 4 days. After filtering the dark purple solution through a plug of silica gel using DCM as eluent and removing the solvent under reduced pressure, the crude solid was triturated with *n*-hexane (2 × 20 mL). The product was dried *in vacuo*, giving $^{i\text{Pr-Anth}}$DPM-H as a purple powder (3.79 g, 5.42 mmol, 84 %). ^{1}H NMR (C_6D_6, 600 MHz, 298 K): δ = 8.09 (br s, 8H, anthracene-aryl-*H*), 7.18 – 7.10 (m, 8H, anthracene-aryl-*H*), 6.89 (s, 2H, Mes-aryl-*H*), 6.75 (d, *J* = 4.2 Hz, 2H, pyrrole-*H*), 6.37 (d, *J* = 4.1 Hz, 2H, pyrrole-*H*), 4.21 – 4.18 (m, 2H, *CH*(CH_3)$_2$), 2.42 (s, 6H, *ortho*-C_6H_2(*CH*$_3$)$_3$), 2.27 (s, 3H, *para*-C_6H_2(*CH*$_3$)$_3$), 1.48 (d, *J* = 6.6 Hz, 12H, CH(*CH*$_3$)$_2$) ppm (N*H* proton not found). ^{1}H NMR (CD_2Cl_2, 600 MHz, 298 K): δ = 8.30 – 8.26 (m, 4H, anthracene-aryl-*H*), 7.83 (d, *J* = 7.8 Hz, 4H, anthracene-aryl-*H*), 7.33 – 7.29 (m, 8H, anthracene-aryl-*H*), 6.89 (s, 2H, Mes-aryl-*H*), 6.87 (br s, 2H, pyrrole-*H*), 6.70 (br s, 2H, pyrrole-*H*), 4.43 (sept, *J* = 7.3 Hz, 2H, C*H*(CH_3)$_2$), 2.47 (s, 3H, *para*-C_6H_2(C*H*$_3$)$_3$), 2.41 (s, 6H, *ortho*-C_6H_2(C*H*$_3$)$_3$), 1.61 (d, *J* = 7.3 Hz, 12H, CH(C*H*$_3$)$_2$) ppm (N*H* proton not found). ^{13}C{^{1}H} NMR (CD_2Cl_2, 151 Hz, 298 K): δ = 154.9 (pyrrole-*C*), 143.8 (anthracene-aryl-*C*), 139.1 (Mes-aryl-*C*), 137.6 (Mes-aryl-*C*), 134.5 (Mes-aryl-*C*), 131.1 (anthracene-aryl-*C*), 129.5 (Mes-aryl-*C*), 129.0 (anthracene-aryl-*C*), 128.7 (anthracene-aryl-*C*H), 128.6 (pyrrole-*C*), 127.4 (pyrrole-*C*H), 126.1 (anthracene-aryl-*C*H), 125.8 (pyrrole-*C*), 125.0 (anthracene-aryl-*C*), 121.8 (pyrrole-*C*H), 29.0 (*C*H(CH_3)$_2$), 23.1 (CH(*C*H$_3$)$_2$), 21.5 (C_6H_2(*C*H$_3$)$_3$), 20.5 (C_6H_2(*C*H$_3$)$_3$) ppm.

4.2.4. (^{Mes}DPM)Na

^{Mes}DPM-H (1.00 g, 2.01 mmol, 1.00 eq.) was dissolved in benzene (30 mL) in a Schlenk tube and sodium *bis*(trimethylsilyl)amide (NaN'') (405 mg, 2.21 mmol, 1.10 eq.) was added. The orange solution was stirred at room temperature for 5 days (temperature increase led to side-products). The solvent was removed under reduced pressure and the solid was dried *in vacuo* to give (^{Mes}DPM)Na as an orange powder in quantitative yield (1.04 g, 2.00 mmol, 99 %). Orange crystals suitable for X-ray diffraction were grown from a saturated benzene solution at room temperature. ^{1}H NMR (C_6D_6, 600 MHz, 298 K): δ = 6.92 (d, *J* = 3.8 Hz, 2H, pyrrole-*H*), 6.89 (s, 6H, aryl-*H*), 6.38 (d, *J* = 3.8 Hz, 2H, pyrrole-*H*), 2.44 (s, 6H, C_6H_2(*CH*$_3$)$_3$), 2.28 (s, 12H, *ortho*-C_6H_2(*CH*$_3$)$_3$), 2.26 (s, 3H, *para*-C_6H_2(*CH*$_3$)$_3$), 2.24 (s, 6H, C_6H_2(*CH*$_3$)$_3$) ppm. ^{13}C{^{1}H} NMR (C_6D_6, 151 MHz, 298 K): δ = 159.0 (pyrrole-*C*), 147.7 (Mes-aryl-*C*), 142.4 (Mes-pyrrole-*C*), 140.2 (pyrrole-*C*), 137.6 (Mes-aryl-*C*), 137.5 (Mes-aryl-*C*), 137.1 (Mes-aryl-*C*), 136.5 (Mes-aryl-*C*), 136.1 (Mes-aryl-*C*), 131.9 (pyrrole-*C*H), 128.6 (Mes-aryl-*C*H), 128.5 (Mes-aryl-*C*H), 127.8 (Mes-aryl-*C*H), 117.8 (pyrrole-*C*H), 21.3 (C_6H_2(*C*H$_3$)$_3$), 21.1 (C_6H_2(*C*H$_3$)$_3$), 20.9 (C_6H_2(*C*H$_3$)$_3$), 20.6 (C_6H_2(*C*H$_3$)$_3$) ppm.

4.2.5. (^{DIPP}DPM)K

^{DIPP}DPM-H (400 mg, 686 μmol, 1.00 eq.) was dissolved in benzene (40 mL) in a Schlenk tube and potassium *bis*(trimethylsilyl)amide (KN'') (205 mg, 1.03 mmol, 1.20 eq.) was added. The red solution was stirred at 50 °C for 3 days. The solvent was removed under reduced pressure and the solid was dried *in vacuo* to give (^{DIPP}DPM)K as a red powder in quantitative yield. Red crystals suitable for X-ray diffraction were grown from a saturated toluene solution which was layered with hexanes and *n*-pentane at −35 °C (288 mg, 464 μmol, 67 %). ^{1}H NMR (C_6D_6, 600 MHz, 298 K): δ = 7.26 (t, *J* = 7.7 Hz, 2H, Dipp-aryl-*H*), 7.06 – 7.01 (m, 4H, Dipp-aryl-*H*), 6.93 (d, *J* = 3.8 Hz, 2H, pyrrole-*H*), 6.88 (s, 2H, Mes-aryl-*H*), 6.41 (d, *J* = 3.7 Hz, 2H, pyrrole-*H*), 3.27 (sept, *J* = 6.8 Hz, 4H, C*H*(CH_3)$_2$), 2.44 (s, 6H, *ortho*-C_6H_2(C*H*$_3$)$_3$), 2.24 (s, 3H, *para*-C_6H_2(C*H*$_3$)$_3$), 1.15 (d, *J* = 6.8 Hz, 12H, CH(C*H*$_3$)$_2$), 1.03 (d, *J* = 6.8 Hz, 12H, CH(C*H*$_3$)$_2$) ppm. ^{13}C{^{1}H} NMR (C_6D_6, 151 MHz, 298 K): δ = 157.4 (pyrrole-*C*), 148.6 (Dipp-aryl-*C*), 148.2 (Mes-aryl-*C*), 142.3 (pyrrole-*C*), 140.3 (toluene-aryl-*C*), 138.8 (Mes-aryl/pyrrole-*C*), 137.9 (Mes-aryl/pyrrole-*C*), 135.9 (toluene-aryl-*C*), 130.9 (Dipp-aryl-*C*H), 129.3 (Mes-aryl-*C*H), 128.6 (toluene-aryl-*C*H), 128.4 (toluene-aryl-*C*H), 128.1 (toluene-aryl-*C*H), 127.8 (toluene-aryl-*C*H), 127.6 (Mes-aryl/pyrrole-*C*), 125.7 (pyrrole-*C*H), 122.9 (Dipp-aryl-*C*H), 117.6 (pyrrole-*C*H), 30.5 (*C*H(CH_3)$_2$), 24.9 CH(*C*H$_3$)$_2$, 24.6 CH(*C*H$_3$)$_2$, 21.4 (C_6H_2(*C*H$_3$)$_3$), 21.3 (C_6H_2(*C*H$_3$)$_3$), 20.6 (C_6H_2(*C*H$_3$)$_3$) ppm.

4.2.6. ($^{iPr\text{-}Anth}$DPM)Na

$^{i\text{Pr-Anth}}$DPM-H (1.00 g, 1.43 mmol, 1.00 eq.) was suspended in benzene (30 mL) in a Schlenk tube. Sodium *bis*(trimethylsilyl)amide (NaN'') (538 mg, 2.94 mmol, 2.05 eq.) was added to the purple suspension and an immediate color change to pink was observed. After stirring the reaction mixture at room temperature overnight, the solvent was removed under reduced pressure and the purple precipitate was triturated with hexanes (2 x 15 mL). After drying the solid *in vacuo*, ($^{i\text{Pr-Anth}}$DPM)Na was isolated as a purple powder (1021 mg, 1.42 mmol, 99 %). Purple crystals suitable for X-ray diffraction were grown from a saturated benzene/THF

solution at room temperature. ^{1}H NMR (C_6D_6, 600 MHz, 298 K): δ = 8.67 (d, J = 8.5 Hz, 4H, anthracene-aryl-*H*), 8.35 (br s, 4H, anthracene-aryl-*H*), 7.28 – 7.22 (m, 10H, anthracene-aryl-*H*, pyrrole-*H*), 6.97 (s, 2H, Mes-aryl-*H*), 6.77 (d, J = 3.4 Hz, 2H, pyrrole-*H*), 4.42 (sept, J = 7.3 Hz, 2H, C*H*(CH_3)$_2$), 2.64 (s, 6H, *ortho*-C_6H_2(CH_3)$_3$), 2.31 (s, 3H, *para*-C_6H_2(CH_3)$_3$), 1.62 (d, J = 7.1 Hz, 12H, CH(CH_3)$_2$) ppm. ^{13}C{^{1}H} NMR (C_6D_6, 151 MHz, 298 K): δ = 157.6 (pyrrole-*C*), 148.7 (Mes-aryl-*C*), 143.7 (anthracene-aryl-*C*), 140.1 (Mes-aryl-*C*), 140.0 (anthracene-aryl-*C*), 137.3 (pyrrole-*C*), 136.4 (pyrrole-*C*), 135.1 (anthracene-aryl-*C*), 132.1 (pyrrole-*C*H), 131.7 (anthracene-aryl-*C*), 129.9 (anthracene-aryl-*C*), 129.1 (aryl-*C*H), 128.6 (Mes-aryl-*C*), 128.4 (anthracene-aryl-*C*H), 128.0 (anthracene-aryl-*C*H), 125.1 (anthracene-aryl-*C*H), 121.5 (pyrrole-*C*H), 28.6 (*C*H(CH_3)$_2$), 22.8 (CH(*C*H_3)$_2$), 21.3 (C_6H_2(*C*H_3)$_3$), 21.0 (C_6H_2(*C*H_3)$_3$) ppm.

4.2.7. (^{Mes}DPM)GaI$_2$

To a solution of (^{Mes}DPM)Na (539 mg, 1.04 mmol, 1.00 eq.) in benzene (15 mL) in a Schlenk tube was added GaI_3 (467 mg, 1.04 mmol, 1.00 eq.) and the reaction mixture was left at room temperature overnight. After filtering the suspension, the solvent was removed under reduced pressure and the red precipitate was dried *in vacuo* yielding (^{Mes}DPM)GaI_2 as a red powder (627 mg, 763 μmol, 73 %). Orange crystals suitable for X-ray diffraction were grown from a saturated toluene solution at −30 °C. ^{1}H NMR (C_6D_6, 600 MHz, 298 K): δ = 6.77 (s, 4H, aryl-*H*), 6.76 (s, 2H, aryl-*H*), 6.62 (d, J = 4.2 Hz, 2H, pyrrole-*H*), 5.98 (d, J = 4.2 Hz, 2H, pyrrole-*H*), 2.33 (s, 12H, *ortho*-C_6H_2(CH_3)$_3$), 2.20 (s, 3H, *para*-C_6H_2(CH_3)$_3$), 2.17 (s, 6H, *ortho*-C_6H_2(CH_3)$_3$), 2.05 (s, 6H, *para*-C_6H_2(CH_3)$_3$) ppm. ^{13}C{^{1}H} NMR (C_6D_6, 151 MHz, 298 K): δ = 163.6 (pyrrole-*C*), 145.9 (Mes-aryl-*C*), 139.5 (Mes-aryl-*C*), 138.4 (pyrrole-*C*), 137.9 (Mes-aryl-*C*), 137.7 (Mes-aryl-*C*), 136.9 (pyrrole-*C*), 134.0 (pyrrole-*C*H), 133.7 (Mes-aryl-*C*), 129.8 (Mes-aryl-*C*), 128.9 (Mes-aryl-*C*H), 128.4 (Mes-aryl-*C*H), 128.2 (Mes-aryl-*C*), 128.1 (Mes-aryl-*C*), 127.9 (Mes-aryl-*C*), 121.4 (pyrrole-*C*H), 22.0 (*ortho*-C_6H_2(*C*H_3)$_3$), 21.3 (*para*-C_6H_2(*C*H_3)$_3$), 21.2 (*ortho*-C_6H_2(*C*H_3)$_3$), 20.1 (*para*-C_6H_2(*C*H_3)$_3$) ppm. Elemental Analysis: Calculated values (%) for $C_{36}H_{37}N_2GaI_2$ (821.24 g/mol): C 52.65, H 4.54, N 3.41; Found (%): C 52.82, H 4.76, N 2.97.

4.2.8. (^{DIPP}DPM)GaI$_2$

To a solution of (^{DIPP}DPM)K (305 mg, 491 μmol, 1.00 eq.) in benzene (10 mL) in a Schlenk tube was added GaI_3 (221 mg, 491 μmol, 1.00 eq.) and an immediate color change from orange to dark red was observed. The reaction was stirred at room temperature overnight. The mixture was filtered, the solvent was removed under reduced pressure, and the precipitate was dried *in vacuo* to obtain (^{DIPP}DPM)GaI_2 as a red powder (393 mg, 434 μmol, 88 %). Orange crystals suitable for X-ray diffraction were grown from a saturated benzene solution by vapor diffusion with *n*-pentane at room temperature. ^{1}H NMR (C_6D_6, 600 MHz, 298 K): δ = 7.26 (d, J = 7.8 Hz, 2H, Dipp-aryl-*H*), 7.12 (d, J = 7.7 Hz, 4H, Dipp-aryl-*H*), 6.75 (s, 2H, Mes-aryl-*H*), 6.68 (d, J = 4.1 Hz, 2H, pyrrole-*H*), 6.29 (d, J = 4.0 Hz, 2H, pyrrole-*H*), 3.00 (sept, J = 6.5 Hz, 4H, C*H*(CH_3)$_2$), 2.23 (s, 6H, *ortho*-C_6H_2(CH_3)$_3$), 2.18 (s, 3H, *para*-C_6H_2(CH_3)$_3$), 1.46 (d, J = 6.7 Hz, 12H, CH(CH_3)$_2$), 1.07 (d, J = 6.9 Hz, 12H, CH(CH_3)$_2$) ppm. ^{13}C{^{1}H} NMR (C_6D_6, 151 MHz, 298 K): δ = 162.8 (pyrrole-*C*), 148.5 (Dipp-aryl-*C*), 138.4 (pyrrole-*C*), 137.1 (pyrrole-*C*), 133.6 (pyrrole-*C*H), 133.5 (Mes-aryl-*C*), 130.8 (Dipp-aryl-*C*H), 130.4 (Dipp-aryl-*C*), 128.6 (Mes-aryl-*C*), 128.4 (Mes-aryl-*C*H), 128.4 (Mes-aryl-*C*), 123.2 (Dipp-aryl-*C*H), 123.1 (pyrrole-*C*H), 31.6 (*C*H(CH_3)$_2$), 26.2 (CH(*C*H_3)$_2$), 23.7 (CH(*C*H_3)$_2$), 21.2 (C_6H_2(*C*H_3)$_3$), 20.4 (C_6H_2(*C*H_3)$_3$) ppm. Elemental Analysis: Calculated values (%) for $C_{42}H_{49}N_2GaI_2$ (905.40 g/mol): C 55.72, H 5.46, N 3.09; Found (%): C 55.35, H 5.96, N 3.43.

4.2.9. ($^{iPr\text{-}Anth}$DPM)GaI$_2$

To a purple solution of ($^{iPr\text{-}Anth}$DPM)Na (472 mg, 655 μmol, 1.00 eq.) in benzene (15 mL) in a Schlenk tube was added GaI_3 (295 mg, 655 μmol, 1.00 eq.) and an immediate color change to pink was observed. The reaction was left at room temperature overnight. After filtering the mixture, the solvent was removed under reduced pressure and the precipitate was dried *in vacuo* yielding ($^{iPr\text{-}Anth}$DPM)GaI_2 as a purple powder (436 mg, 427 μmol, 65 %). Purple crystals suitable for X-ray diffraction were grown from a saturated benzene/hexanes solution layered with Et_2O at room temperature. ^{1}H NMR (C_6D_6, 600 MHz, 298 K): δ = 8.22 (br s, 4H, anthracene-aryl-*H*), 7.89 (d, J = 8.3 Hz, 4H, anthracene-aryl-*H*), 7.15 – 7.10 (m, 8H, anthracene-aryl-*H*), 6.86 (s, 2H, Mes-aryl-*H*), 6.84 (d, J = 4.2 Hz, 2H, pyrrole-*H*), 6.35 (d, J = 4.2 Hz, 2H, pyrrole-*H*), 4.27 (sept, J = 7.4 Hz, 2H, C*H*(CH_3)$_2$), 2.43 (s, 6H, *ortho*-C_6H_2(CH_3)$_3$), 2.26 (s, 3H, *para*-C_6H_2(CH_3)$_3$), 1.50 (d, J = 7.3 Hz, 12H, CH(CH_3)$_2$) ppm. ^{1}H NMR (C_6D_6/THF-d_8, 600 MHz, 298 K): δ = 8.22 (br s, 4H, anthracene-aryl-*H*), 7.80 – 7.78 (m, 4H, anthracene-aryl-*H*), 7.14 – 7.12 (m, 8H, anthracene-aryl-*H*), 6.90 (s, 2H, Mes-aryl-*H*), 6.84 (d, J = 4.1 Hz, 2H, pyrrole-*H*), 6.39 (d, J = 4.1 Hz, 2H, pyrrole-*H*), 4.29 (sept, J = 7.4 Hz, 2H, C*H*(CH_3)$_2$), 2.40 (s, 6H, *ortho*-C_6H_2(CH_3)$_3$), 2.28 (s, 3H, *para*-C_6H_2(CH_3)$_3$), 1.50 (d, J = 7.2 Hz, 12H, CH(CH_3)$_2$) ppm. ^{13}C{^{1}H} NMR (C_6D_6/THF-d_8, 151 MHz, 298 K): δ = 162.3 (pyrrole-*C*), 146.7 (Mes-aryl-*C*), 144.0 (anthracene-aryl-*C*), 138.7 (pyrrole-*C*), 138.5 (pyrrole-*C*), 137.2 (Mes-aryl-*C*), 133.9 (pyrrole-*C*H), 133.7 (Mes-aryl-*C*), 132.1 (anthracene-aryl-*C*), 129.4 (anthracene-aryl-*C*), 128.8 (anthracene-aryl-*C*H), 128.6 (Mes-aryl-*C*H), 128.5 (anthracene-aryl-*C*), 128.3 (anthracene-aryl-*C*), 126.0 (anthracene-aryl-*C*), 125.7 (anthracene-aryl-*C*H), 123.7 (pyrrole-*C*H), 28.9 (*C*H(CH_3)$_2$), 22.9 (CH(*C*H_3)$_2$), 21.2 (C_6H_2(*C*H_3)$_3$), 20.6 (C_6H_2(*C*H_3)$_3$) ppm. Elemental Analysis: Calculated values (%) for $C_{52}H_{45}N_2GaI_2$ (1021.48 g/mol): C 61.14, H 4.44, N 2.74; Found (%): C 63.03, H 4.72, N 2.59. Although these results are outside the range viewed as establishing analytical purity, they are provided to illustrate the best values obtained to date.

4.2.10. (^{DIPP}DPM)Ga

(^{DIPP}DPM)GaI_2 (30 mg, 33.1 μmol, 1.00 eq.) was dissolved in benzene-d_6 (600 μL) in a Schlenk tube. KC_8 (9.18 mg, 67.9 μmol, 2.05 eq.) was added to the solution. The reaction mixture was stirred at 50 °C for 3 days. The mixture was filtered, the solvent was removed under reduced pressure, and the precipitate was dried *in vacuo* to obtain (^{DIPP}DPM)Ga as a dark red powder in quantitative yield. Dark red crystals suitable for X-ray diffraction were grown from a saturated hexanes solution at −35 °C (8.00 mg, 12.3 μmol, 37 %). ^{1}H NMR (C_6D_6, 600 MHz, 298 K): δ = 7.29 (t, J = 7.8 Hz, 4H, Dipp-aryl-*H*), 7.13 (s, 1H, Dipp-aryl-*H*), 7.11 (s, 1H, Dipp-aryl-*H*), 6.79 (s, 2H, Mes-aryl-*H*), 6.71 (d, J = 3.9 Hz, 2H, pyrrole-*H*), 6.31 (d, J = 3.9 Hz, 2H, pyrrole-*H*), 3.03 (sept, J = 6.8 Hz, 4H, C*H*(CH_3)$_2$), 2.22 (s, 6H, *ortho*-C_6H_2(CH_3)$_3$), 2.19 (s, 3H, *para*-C_6H_2(CH_3)$_3$), 1.21 (d, J = 6.9 Hz, 12H, CH(CH_3)$_2$), 1.12 (d, J = 6.9 Hz, 12H, CH(CH_3)$_2$) ppm. ^{13}C{^{1}H} NMR (C_6D_6, 151 MHz, 298 K): δ = 162.3 (pyrrole-*C*), 148.3 (Dipp-aryl-*C*), 137.2 (pyrrole-*C*), 130.6 (pyrrole-*C*H), 129.7 (Dipp/Mes-aryl-*C*H), 128.5 (Dipp-aryl-*C*), 128.4 (Mes-aryl-*C*H), 128.2 (Dipp-aryl-*C*H), 128.1 (Mes-aryl-*C*), 127.9 (Mes-aryl-*C*), 127.6 (pyrrole-*C*), 122.9 (Dipp-*C*H), 120.5 (pyrrole-*C*H), 31.5 (*C*H(CH_3)$_2$), 25.1 (CH(*C*H_3)$_2$), 23.8 (CH(*C*H_3)$_2$), 21.2 (C_6H_2(*C*H_3)$_3$), 20.2 (C_6H_2(*C*H_3)$_3$) ppm. Elemental Analysis: Calculated values (%) for $C_{42}H_{49}N_2Ga$ (651.59 g/mol): C 77.42, H 7.58, N 4.30; Found (%): C 75.45, H 7.66, N 3.73. Although these results are outside the range viewed as establishing analytical purity, they are provided to illustrate the best values obtained to date.

4.2.11. ($^{iPr\text{-}Anth}$DPM)Ga

($^{iPr\text{-}Anth}$DPM)GaI_2 (30.0 mg, 29.4 μmol, 1.00 eq.) was dissolved in benzene-d_6 (600 μL) in a Schlenk tube. KC_8 (8.14 mg, 60.2 μmol, 2.05 eq.) was added to the purple solution. The reaction mixture was stirred at 50 °C for 17 h. The reaction mixture was filtered, the solvent was removed under reduced pressure, and the precipitate was dried *in vacuo* to obtain ($^{iPr\text{-}Anth}$DPM)Ga as a dark purple powder. Any attempt to crystallize this complex from a variety of solvents failed. ^{1}H NMR (THF-d_8, 600 MHz, 298 K): δ = 8.39 (d, J = 7.5 Hz, 4H, anthracene-aryl-*H*), 7.82 (d, J = 8.5 Hz, 4H, anthracene-aryl-*H*), 7.34 – 7.32 (m, 6H,

anthracene-aryl-*H*), 7.28 – 7.27 (m, 2H, anthracene-aryl-*H*), 7.10 (s, 2H, Mes-aryl-*H*), 6.76 (d, $J = 3.8$ Hz, 2H, pyrrole-*H*), 6.47 (d, $J = 3.8$ Hz, 2H, pyrrole-*H*), 4.55 (sept, $J = 7.5$ Hz, 2H, C*H*$(CH_3)_2$), 2.43 – 2.42 (m, 9H, $C_6H_2(CH_3)_3$), 1.66 (d, $J = 7.2$ Hz, 12H, CH(C*H*$_3)_2$) ppm. $^{13}C\{^1H\}$ NMR (THF-d_8, 151 MHz, 298 K): $\delta = 160.9$ (pyrrole-*C*), 147.7 (Mes-aryl-*C*), 142.6 (anthracene-aryl-*C*), 138.7 (pyrrole-*C*), 138.5 (anthracene-aryl-*C*), 137.9 (anthracene-aryl-*C*), 137.7 (pyrrole-*C*), 136.4 (anthracene-aryl-*C*), 135.0 (anthracene-aryl-*C*), 132.8 (anthracene-aryl-*C*), 130.9 (pyrrole-*C*H), 130.3 (anthracene-aryl-*C*), 129.9 (Mes-aryl-*C*), 129.0 (anthracene-aryl-*C*), 128.8 (Mes-aryl-*C*H), 128.7 (anthracene-aryl-*C*H), 128.4 (anthracene-aryl-*C*), 125.9 (anthracene-aryl-*C*H), 125.8 (anthracene-aryl-*C*H), 122.5 (pyrrole-*C*H), 29.4 (*C*H$(CH_3)_2$), 23.3 (CH(*C*H$_3)_2$), 23.2 (CH(*C*H$_3)_2$), 21.5 ($C_6H_2(CH_3)_3$), 20.6 ($C_6H_2(CH_3)_3$) ppm. Elemental Analysis: Calculated values (%) for $C_{52}H_{45}N_2Ga$ (767.67 g/mol): C 81.36, H 5.91, N 3.65; Found (%): C 79.84, H 5.72, N 3.51. Although these results are outside the range viewed as establishing analytical purity, they are provided to illustrate the best values obtained to date.

4.2.12. ($^{iPr\text{-}Anth}$DPM)Ga(N_3)N($SiMe_3$)$_2$

($^{iPr\text{-}Anth}$DPM)Ga (20.3 mg, 26.5 μmol, 1.00 eq.) was dissolved in benzene-d_6 (600 μL) in a J.-Young NMR tube. Trimethylsilyl azide (6.11 mg, 53.0 μmol, 2.00 eq.) was added at room temperature. The reaction was finished immediately as indicated by ^{1}H NMR spectroscopy. The solvent was removed under reduced pressure, and the residue was dried *in vacuo* to obtain ($^{iPr\text{-}Anth}$DPM)Ga(N_3)($NTMS_2$) as a purple powder in quantitative yield. Purple crystals suitable for X-ray diffraction analysis were grown from a saturated toluene solution by vapor diffusion with Et_2O and *n*-pentane at −35 °C (8.20 mg, 8.45 μmol, 32 %). ^{1}H NMR (C_6D_6, 600 MHz, 298 K): $\delta = 8.30$ (d, $J = 41.1$ Hz, 4H, anthracene-aryl-*H*), 8.20 (d, $J = 8.6$ Hz, 2H, anthracene-aryl-*H*), 7.97 – 7.96 (m, 2H, anthracene-aryl-*H*), 7.72 – 7.70 (m, 2H, anthracene-aryl-*H*), 7.24 – 7.18 (m, 6H, anthracene-aryl-*H*), 6.88 (s, 1H, Mes-aryl-*H*), 6.84 (d, $J = 4.2$ Hz, 2H, pyrrole-*H*), 6.82 (s, 1H, Mes-aryl-*H*), 6.28 (d, $J = 4.2$ Hz, 2H, pyrrole-*H*), 4.37 (sept, $J = 7.1$ Hz, 2H, C*H*$(CH_3)_2$), 2.54 (s, 3H, *ortho*-$C_6H_2(CH_3)_3$), 2.45 (s, 3H, *ortho*-$C_6H_2(CH_3)_3$), 2.25 (s, 3H, *para*-$C_6H_2(CH_3)_3$), 1.61 (dd, $J = 7.1$, 5.0 Hz, 12H, CH(C*H*$_3)_2$), −0.33 (s, 9H, TMS-C*H*$_3$), −1.36 (s, 9H, TMS-C*H*$_3$) ppm. $^{13}C\{^1H\}$ NMR (C_6D_6, 151 MHz, 298 K): $\delta = 161.9$ (pyrrole-*C*), 146.7 (Mes-aryl-*C*), 143.5 (anthracene-aryl-*C*), 139.9 (pyrrole-*C*), 138.3 (Mes-aryl-*C*), 137.9 (Mes-aryl-*C*), 137.8 (anthracene-aryl-*C*), 136.6 (pyrrole-*C*), 134.9 (anthracene-aryl-*C*), 133.8 (anthracene-aryl-*C*H), 132.8 (anthracene-aryl-*C*), 131.7 (anthracene-aryl-*C*), 130.1 (anthracene-aryl-*C*), 129.4 (anthracene-aryl-*C*), 129.3 (anthracene-aryl-*C*), 128.7 (pyrrole-*C*H), 128.6 (Mes-aryl-*C*H), 127.8 (anthracene-aryl-*C*), 127.6 (anthracene-aryl-*C*), 125.9 (anthracene-aryl-*C*H), 125.7 (anthracene-aryl-*C*), 125.3 (anthracene-aryl-*C*H), 125.1 (pyrrole-*C*H), 34.4 (CH(*C*H$_3)_2$), 28.8 (*C*H$(CH_3)_2$), 22.9 (CH(*C*H$_3)_2$), 22.9 (CH(*C*H$_3)_2$), 22.7 (CH(*C*H$_3)_2$), 21.4 (CH(*C*H$_3)_2$), 21.2 ($C_6H_2(CH_3)_3$), 20.5 ($C_6H_2(CH_3)_3$), 20.2 ($C_6H_2(CH_3)_3$), 15.6 (CH(*C*H$_3)_2$), 14.3 (CH(*C*H$_3)_2$), 5.2 (TMS-*C*H$_3$), 3.4 (TMS-*C*H$_3$) ppm. ^{29}Si NMR (C_6D_6, 119 MHz, 298 K): $\delta = 3.83$ (TMS), 0.87 (TMS) ppm. Elemental Analysis: Calculated values (%) for $C_{58}H_{63}N_6GaSi_2$ (970.08 g/mol): C 71.81, H 6.55, N 8.66; Found (%): C 70.44, H 6.03, N 6.98. Although these results are outside the range viewed as establishing analytical purity, they are provided to illustrate the best values obtained to date.

4.2.13. (^{DIPP}DPM)Ga[$N_4(SiMe_3)_2$]

(^{DIPP}DPM)Ga (21.3 mg, 32.7 μmol, 1.00 eq.) was dissolved in benzene-d_6 (600 μL) in a J.-Young NMR tube. Trimethylsilyl azide (7.53 mg, 65.4 μmol, 2.00 eq.) was added at room temperature. The reaction was finished immediately as indicated by ^{1}H NMR spectroscopy. The solvent was removed under reduced pressure, and the residue was dried *in vacuo* to obtain (^{DIPP}DPM)Ga(N_4TMS_2) as a red powder in quantitative yield. Red crystals suitable for X-ray diffraction analysis were grown from a saturated methylcyclohexane solution layered with HMDSO at −35 °C (4.20 mg, 4.92 μmol, 15 %). ^{1}H NMR (C_6D_6, 600 MHz, 298 K): $\delta = 7.24$ (t, $J = 7.8$ Hz, 2H, Dipp-aryl-*H*), 7.12 – 7.11 (m, 2H, Dipp-aryl-*H*), 7.08 – 7.05 (m, 2H, Dipp-aryl-*H*), 6.87 (s, 1H, Mes-aryl-*H*), 6.75 (s, 1H, Mes-aryl-*H*), 6.53 (d, $J = 4.1$ Hz, 2H, pyrrole-*H*), 6.16 (d, $J = 4.1$ Hz, 2H, pyrrole-*H*), 2.86 (m, 2H, C*H*$(CH_3)_2$), 2.52 (m, 2H, C*H*$(CH_3)_2$), 2.45 (s, 3H, $C_6H_2(CH_3)_3$), 2.23 (s, 3H, $C_6H_2(CH_3)_3$), 1.98 (s, 3H, $C_6H_2(CH_3)_3$), 1.34 – 1.26 (m, 12H, CH(C*H*$_3)_2$), 1.02 – 0.98 (m, 12H, CH(C*H*$_3)_2$), 0.31 (s, 9H, TMS-C*H*$_3$, overlapping with residual signal of silicone grease), −0.22 (s, 9H, TMS-C*H*$_3$) ppm. $^{13}C\{^1H\}$ NMR (C_6D_6, 151 MHz, 298 K): $\delta = 163.1$ (pyrrole-*C*), 147.7 (Dipp-aryl-*C*), 145.8 (Dipp-aryl-*C*), 140.5 (pyrrole-*C*), 138.3 (Mes-aryl-*C*), 134.3 (Dipp-aryl-*C*H), 133.3 (pyrrole-*C*H), 132.1 (pyrrole-*C*), 130.6 (Dipp-aryl-*C*H), 128.5 (Mes-aryl-*C*), 128.4 (Mes-aryl-*C*H), 127.6 (Mes-aryl-*C*), 125.3 (pyrrole-*C*H), 32.0 (*C*H$(CH_3)_2$), 31.5 (*C*H$(CH_3)_2$), 31.0 (*C*H$(CH_3)_2$), 29.4 (CH(*C*H$_3)_2$), 26.6 (CH(*C*H$_3)_2$), 26.5 (CH(*C*H$_3)_2$), 23.4 (CH(*C*H$_3)_2$), 23.1 (CH(*C*H$_3)_2$), 22.3 ($C_6H_2(CH_3)_3$), 21.1 ($C_6H_2(CH_3)_3$), 14.4 (CH(*C*H$_3)_2$), 11.7 (CH(*C*H$_3)_2$), 1.9 (TMS-*C*H$_3$), 1.1 (TMS-*C*H$_3$) ppm. ^{29}Si NMR (C_6D_6, 119 MHz, 298 K): $\delta = 6.99$ (TMS), 6.48 (TMS) ppm. Elemental Analysis: Calculated values (%) for $C_{48}H_{67}N_6GaSi_2$ (854.00 g/mol): C 67.51, H 7.91, N 9.84; Found (%): C 63.00, H 7.45, N 8.01. Calculated values (%) for $C_{48}H_{67}N_6GaSi_2$ ■ 0.95 HMDSO: C 63.97, H 8.41, N 8.34; Found (%): C 63.00, H 7.45, N 8.01. Although these results are outside the range viewed as establishing analytical purity, they are provided to illustrate the best values obtained to date.

4.3. X-ray diffraction studies

Full details for crystal structure determinations can be found in the Supporting Information. The CIF data of all structures have been deposited with the Cambridge Crystallographic Data Center with the deposition numbers: 2,360,734 (^{DIPP}DPM)K·(toluene), 2,360,735 ($^{iPr\text{-}Anth}$DPM)Na·$(THF)_2$, 2,360,736 (^{Mes}DPM)GaI_2, 2,360,737 (^{DIPP}DPM)GaI_2, 2,360,738 ($^{iPr\text{-}Anth}$DPM)GaI_2, 2,360,739 (^{DIPP}DPM)Ga, 2,360,740 (^{DIPP}DPM)Ga[$N_4(SiMe_3)_2$], 2,360,741 ($^{iPr\text{-}Anth}$DPM)Ga(N_3)N($SiMe_3$)$_2$.

4.4. Computational details

Full details for the DFT calculations can be found in the Supporting Information. This includes the xyz-coordinates of all optimized molecular structures.

CRediT authorship contribution statement

Tim Richter: Writing – original draft, Validation, Investigation, Formal analysis, Data curation, Conceptualization. **Stefan Thum:** Validation, Investigation, Formal analysis, Data curation. **Oliver P.E. Townrow:** Validation, Investigation, Formal analysis, Data curation. **Jens Langer:** Validation, Investigation, Formal analysis, Data curation. **Michael Wiesinger:** Validation, Investigation, Formal analysis, Data curation. **Sjoerd Harder:** Writing – review & editing, Writing – original draft, Validation, Supervision, Resources, Project administration, Funding acquisition, Formal analysis, Conceptualization.

Declaration of competing interest

There are no conflicts to declare.

Data availability

The supporting information includes selected NMR spectra, crystallographic details including ORTEP plots for all crystal structures. Crystallographic data have been deposited with the Cambridge Crystallographic Data centre as supplementary publication numbers: CCDC 2360734–2360741.

Acknowledgement

We acknowledge A. Roth for CHN analyses and Dr. C. Färber and J. Schmidt for assistance with NMR analyses. This research did not receive any specific grant from funding agencies in the public, commercial, or not-for-profit sectors.

Supplementary materials

Supplementary material associated with this article can be found, in the online version, at doi:10.1016/j.jorganchem.2024.123356.

References

[1] M. Asay, C. Jones, M. Driess, *N*-heterocyclic carbene analogues with low-valent group 13 and group 14 elements: syntheses, structures, and reactivities of a new generation of multitalented ligands, Chem. Rev. 111 (2011) 354–396, https://doi.org/10.1021/cr100216y.

[2] M. Zhong, S. Sinhababu, H.W. Roesky, The unique β-diketiminate ligand in aluminum(ɪ) and gallium(ɪ) chemistry, Dalton. Trans. 49 (2020) 1351–1364, https://doi.org/10.1039/C9DT04763H.

[3] M. He, C. Hu, R. Wei, X.-F. Wang, L.L. Liu, Recent advances in the chemistry of isolable carbene analogues with group 13–15 elements, Chem. Soc. Rev. 10 (2024) 1039, https://doi.org/10.1039/D3CS00784G. D3CS00784G.

[4] P.P. Power, Main-group elements as transition metals, NatureNature 463 (2010) 171–177, https://doi.org/10.1038/nature08634.

[5] C. Weetman, S. Inoue, The Road Travelled: after Main-Group Elements as Transition Metals, ChemCatChem 10 (2018) 4213–4228, https://doi.org/10.1002/cctc.201800963.

[6] C. Cui, H.W. Roesky, H.-G. Schmidt, M. Noltemeyer, H. Hao, F. Cimpoesu, Synthesis and Structure of a Monomeric Aluminum(I) Compound [{HC(CMeNAr)2}Al] (Ar=2,6–iPr2C6H3): a Stable Aluminum Analogue of a Carbene, Angew. Chem. 112 (2000) 4444–4446, https://doi.org/10.1002/1521-3757(20001201)112:23<4444::AID−ANGE4444>3.0.CO;2-U.

[7] X. Li, X. Cheng, H. Song, C. Cui, Synthesis of HC[(CBu ^{t})(NAr)] $_{2}$ Al (Ar = 2,6-$Pr^{i}_{2}C_{6}H_{3}$) and Its Reaction with Isocyanides, a Bulky Azide, and $H_{2}O$, Organometallics 26 (2007) 1039–1043, https://doi.org/10.1021/om061107j.

[8] N.J. Hardman, B.E. Eichler, P.P. Power, Synthesis and characterization of the monomer Ga{(NDippCMe)2CH} (Dipp = C6H3Pri2-2,6): a low valent gallium(i) carbene analogue, Chem. Commun. (2000) 1991–1992, https://doi.org/10.1039/b005686n.

[9] O. Kysliak, H. Görls, R. Kretschmer, Salt metathesis as an alternative approach to access aluminium(ɪ) and gallium(ɪ) β-diketiminates, Dalton. Trans. 49 (2020) 6377–6383, https://doi.org/10.1039/D0DT01342K.

[10] S. Grams, J. Mai, J. Langer, S. Harder, Synthesis, Structure, and Reactivity of a Superbulky Low-Valent β-Diketiminate Al(I) Complex, Organometallics. Organometallics. 41 (2022) 2862–2867, https://doi.org/10.1021/acs.organomet.2c00427.

[11] T. Richter, S. Thum, O.P.E. Townrow, M. Wiesinger, J. Langer, Synthesis, structure, and reactivity of a superbulky low-valent b-diketiminate Ga(I) complex, (n.d.).

[12] T. Richter, S. Thum, T. Vilpas, O.P.E. Townrow, L. Klerner, J. Langer, S. Harder, Dipyrromethene as a Ligand for the Stabilization of Low-Valent Gallium Complexes, Organometallics 43 (2024) 1377–1385, https://doi.org/10.1021/acs.organomet.4c00164.

[13] A. Loudet, K. Burgess, BODIPY Dyes and Their Derivatives: syntheses and Spectroscopic Properties, Chem. Rev. 107 (2007) 4891–4932, https://doi.org/10.1021/cr078381n.

[14] N.J. Hardman, C. Cui, H.W. Roesky, W.H. Fink, P.P. Power, Stable, Monomeric Imides of Aluminum and Gallium: synthesis and Characterization of [{HC(MeCDippN)2}MN-2,6-Trip2C6H3] (M=Al or Ga; Dipp=2,6-iPr2C6H3; Trip=2,4,6-iPr3C6H2), Angew. Chem. Int. Ed. 40 (2001) 2172–2174, https://doi.org/10.1002/1521-3773(20010601)40:11<2172::AID−ANIE2172>3.0.CO;2-Y.

[15] R.J. Wright, A.D. Phillips, T.L. Allen, W.H. Fink, P.P. Power, Synthesis and Characterization of the Monomeric Imides Ar‘MNAr“ (M = Ga or In; Ar‘ or Ar“ = Terphenyl Ligands) with Two-Coordinate Gallium and Indium, J. Am. Chem. Soc. 125 (2003) 1694–1695, https://doi.org/10.1021/ja029422u.

[16] R.J. Baker, C. Jones, D.P. Mills, D.M. Murphy, E. Hey-Hawkins, R. Wolf, The reactivity of gallium-(ɪ), -(ɪɪ) and -(ɪɪɪ) heterocycles towards Group 15 substrates: attempts to prepare gallium–terminal pnictinidene complexes, Dalton. Trans. (2006) 64–72, https://doi.org/10.1039/B511451A.

[17] E.R. King, T.A. Betley, C.−.H. Bond, Amination from a Ferrous Dipyrromethene Complex, Inorg. Chem. 48 (2009) 2361–2363, https://doi.org/10.1021/ic900219b.

[18] G. Ballmann, S. Grams, H. Elsen, S. Harder, Dipyrromethene and β-Diketiminate Zinc Hydride Complexes: resemblances and Differences, Organometallics. 38 (2019) 2824–2833, https://doi.org/10.1021/acs.organomet.9b00334.

[19] G. Ballmann, B. Rösch, S. Harder, Stabilization of Heteroleptic Heavier Alkaline Earth Metal Complexes with an Encapsulating Dipyrromethene Ligand, Eur. J. Inorg. Chem. 2019 (2019) 3683–3689, https://doi.org/10.1002/ejic.201900743.

[20] L. Falivene, R. Credendino, A. Poater, A. Petta, L. Serra, R. Oliva, V. Scarano, L. Cavallo, SambVca 2. A Web Tool for Analyzing Catalytic Pockets with Topographic Steric Maps, Organometallics. 35 (2016) 2286–2293, https://doi.org/10.1021/acs.organomet.6b00371.

[21] Q. Yu, L. Zhang, Y. He, J. Pan, H. Li, G. Bian, X. Chen, G. Tan, A stable tetrazagallole and its radical anion dimer, Chem. Commun. 57 (2021) 9268–9271, https://doi.org/10.1039/D1CC03448K.

[22] J. Kretsch, A. Kreyenschmidt, T. Schillmöller, C. Sindlinger, R. Herbst-Irmer, D. Stalke, Group 13 Heavier Carbene Analogues Stabilized by the Bulky Bis(4-benzhydryl-benzoxazol-2-yl)methanide Ligand, Inorg. Chem. 60 (2021) 7389–7398, https://doi.org/10.1021/acs.inorgchem.1c00617.

[23] N.J. Hardman, P.P. Power, Unique structural isomerism involving tetrazole and amide/azide derivatives of gallium, Chem. Commun. (2001) 1184–1185, https://doi.org/10.1039/b100466m.

[24] J.M. Tanko, R.H. Mas, Kinetic *vs*. thermodynamic factors in .alpha.-hydrogen atom abstractions from alkyl aromatics, J. Org. Chem. 55 (1990) 5145–5150, https://doi.org/10.1021/jo00304a029.

[25] F.J.M. Gil, M.A. Salgado, J.M. Gil, On the Synthesis of Triiodides of Aluminium, Gallium and Indium, Synth. React. Inorg. Met.-Org. Chem. 16 (1986) 663–666, https://doi.org/10.1080/00945718608057539.

[26] N. Ji, H. O'Dowd, B.M. Rosen, A.G. Myers, Enantioselective Synthesis of N1999A2, J. Am. Chem. Soc. 128 (2006) 14825–14827, https://doi.org/10.1021/ja0662467.

[27] D.M. Ottmers, H.F. Rase, Potassium graphites prepared by mixed-reaction technique, Carbon. N. Y. 4 (1966) 125–127, https://doi.org/10.1016/0008-6223(66)90017-0.

[28] J. Hicks, M. Juckel, A. Paparo, D. Dange, C. Jones, Multigram Syntheses of Magnesium(I) Compounds Using Alkali Metal Halide Supported Alkali Metals as Dispersible Reducing Agents, Organometallics. 37 (2018) 4810–4813, https://doi.org/10.1021/acs.organomet.8b00803.

[29] R.D. Rieth, N.P. Mankad, E. Calimano, J.P. Sadighi, Palladium-catalyzed cross-coupling of pyrrole anions with aryl chlorides, bromides, and iodides, Org. Lett. 6 (2004) 3981–3983, https://doi.org/10.1021/ol048367m.